



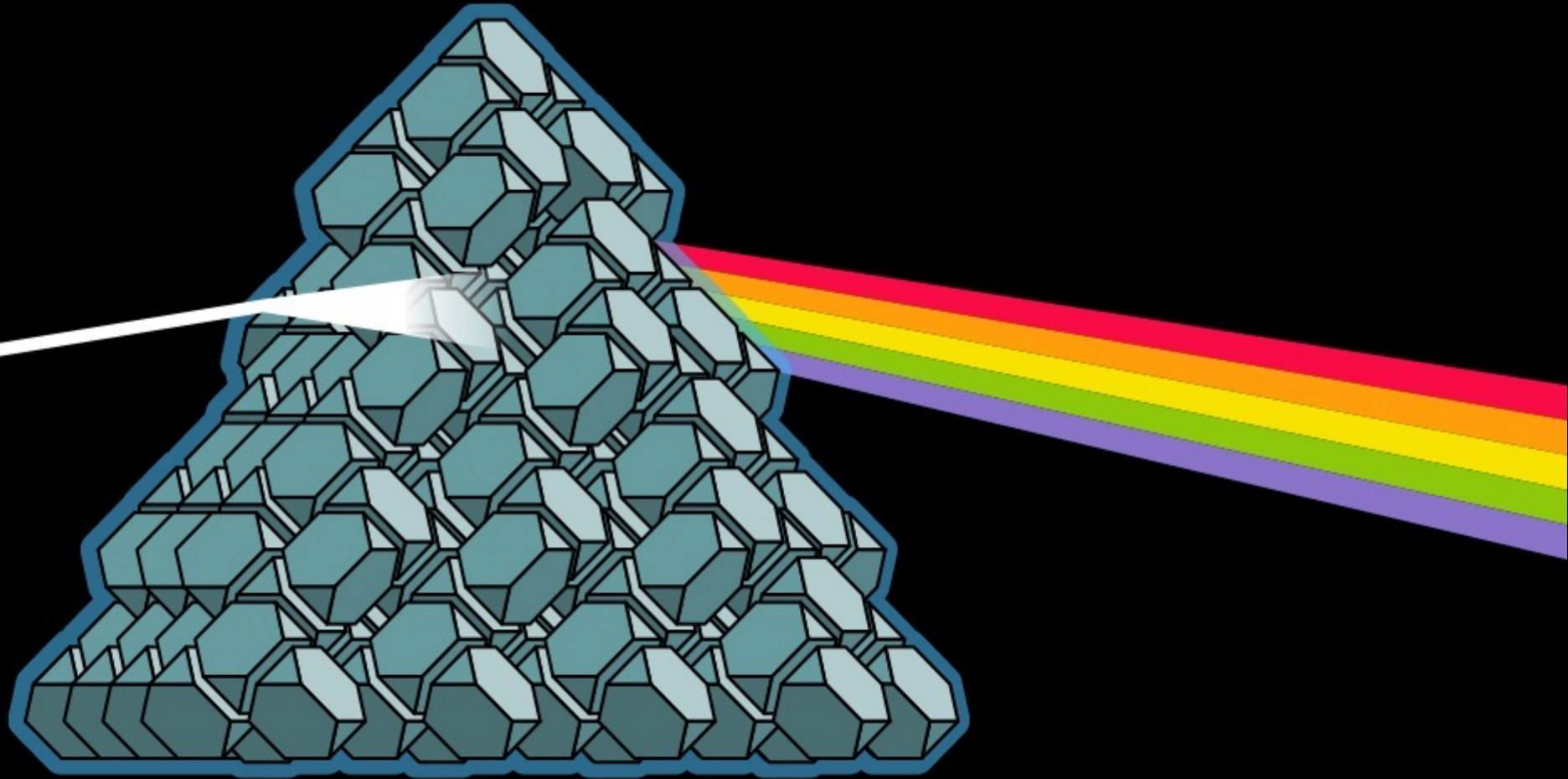
The Search for Novel Mesoscale Materials

Rose K. Cersonsky

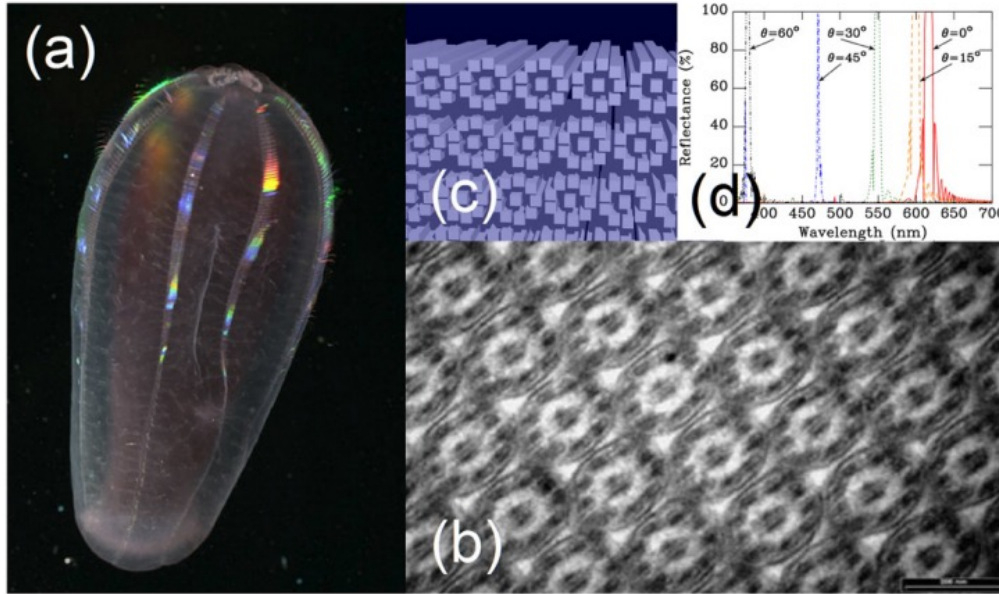
Laboratory of Computational Science and Modeling
(COSMO)

École Polytechnique Fédérale de Lausanne (EPFL)

Lausanne, Switzerland



Designing Nanoparticles for the Self-Assembly of Novel (Photonic) Materials



Optical properties of the iridescent organ of the comb-jellyfish *Beroë cucumis* (Ctenophora)

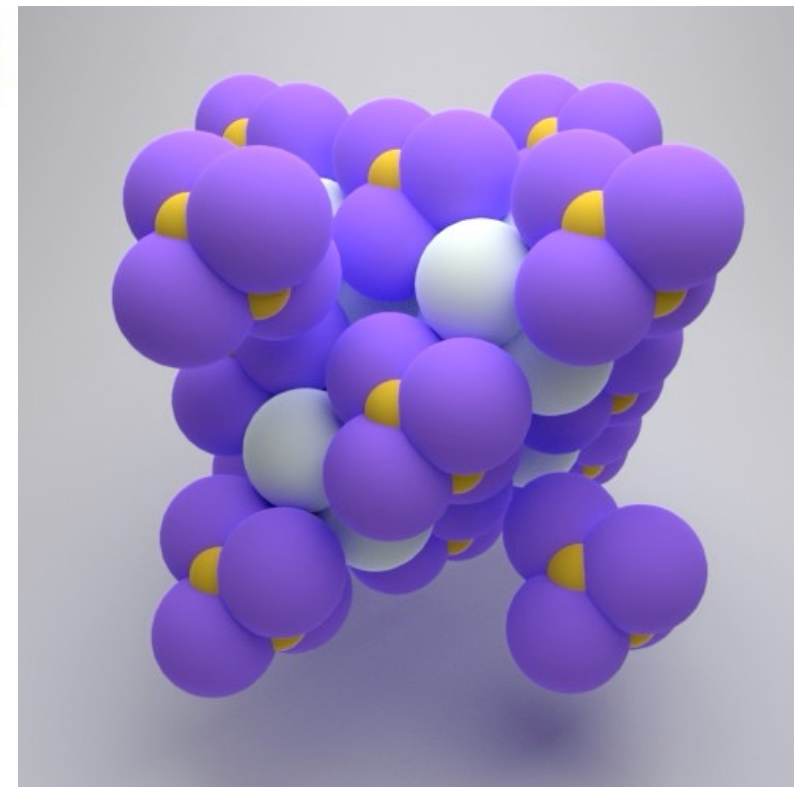
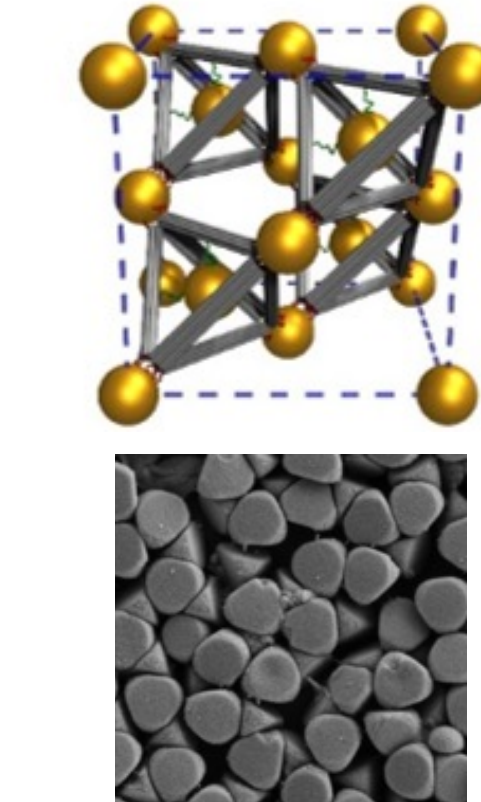
Victoria Welch, et al.
Phys. Rev. E 73, 041916 2006



Optical properties of gyroid structured materials: from photonic crystals to metamaterials

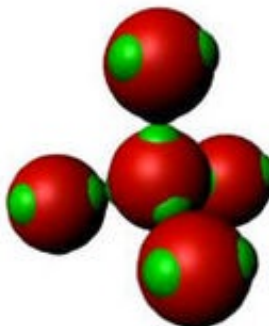
James A. Dolan , et al.
Advanced Optical Materials 3 (1), 12-32

November 7, 2021



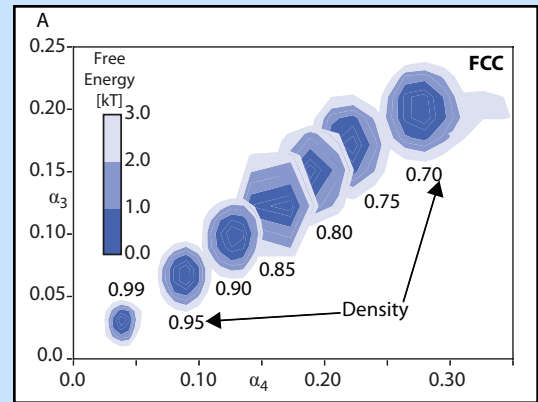
Colloidal Diamond
He, M., et al.
Nature 585, 524-529 (2020).

Diamond family of nanoparticle superlattices
W. Liu, et. al,
Science 351, 582-586 (2016).



Relevance of packing to colloidal self-assembly.

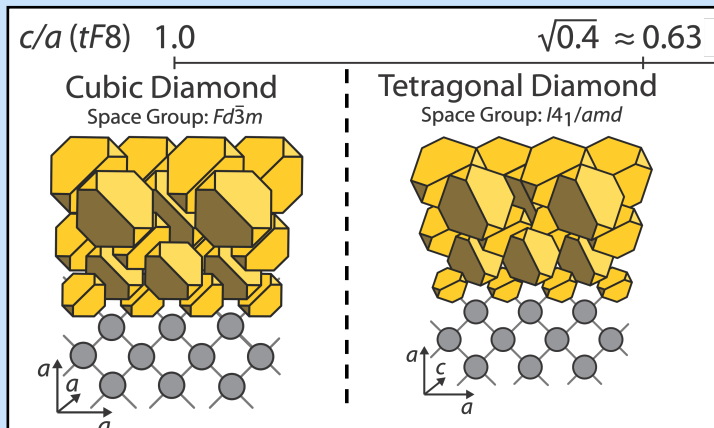
Cersonsky, R. K., van Anders, G., Dodd, P. M., & Glotzer, S. C. (2018). *Proceedings of the National Academy of Sciences*, 115(7), 1439-1444.



- Pauling's packing rules are **not** a causal mechanism for nanoparticle self-assembly
- Using the Digital Alchemy framework, I showed that **adding small imperfections** to nanoparticle shapes would better stabilize nanocrystals

Pressure-Tunable Photonic Band Gaps in an Entropic Colloidal Crystal

Cersonsky, R. K., Dshemuchadse, J., Antonaglia, J., van Anders, G., & Glotzer, S. C. (2018). *Physical Review Materials*, 2(12), 125201.



- Nanoparticles that stabilized diamond in self-assembly can **transition to lower-symmetry derivatives** at high pressure
- Small distortions in diamond **did not destroy the photonic band gap**

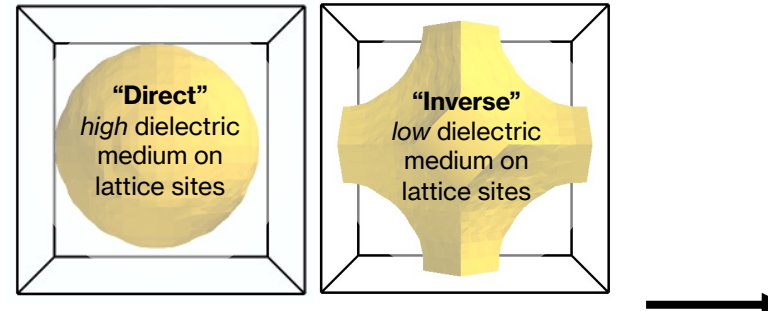
At time of presentation, this manuscript was not yet published, please see rosecersonsky.com for recent publications.

...Small distortions in diamond **did not destroy the photonic band gap...**
...minimal effect on the photonic band structure...

what is the span of crystallographic structures capable of supporting a photonic band gap?

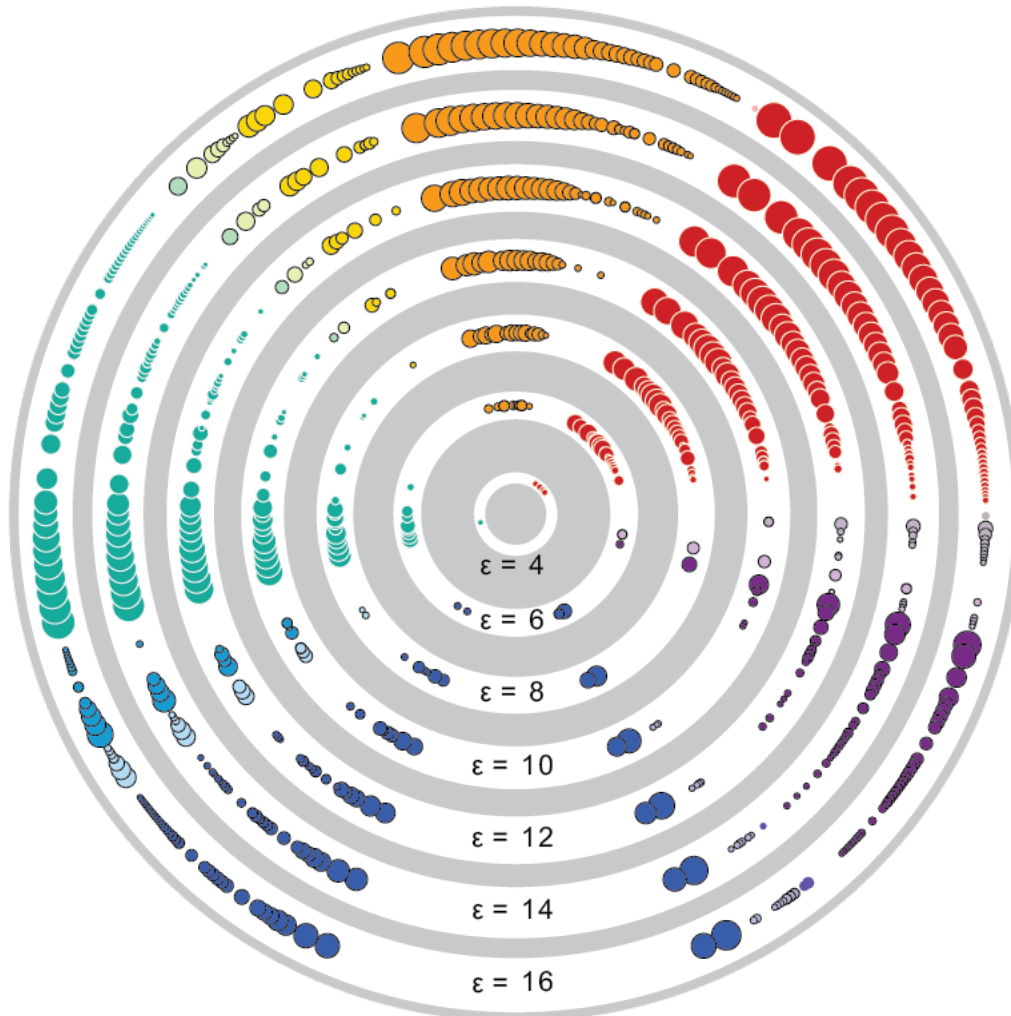


**Scraped 1300 unique
crystal structures from
crystal repositories**



**Ignoring atomic species,
turned each structure into
2 templates with which to
sample multiple
parameters**

**Ran >150,000 band
structure to determine
which “templates”
supported PBGs**



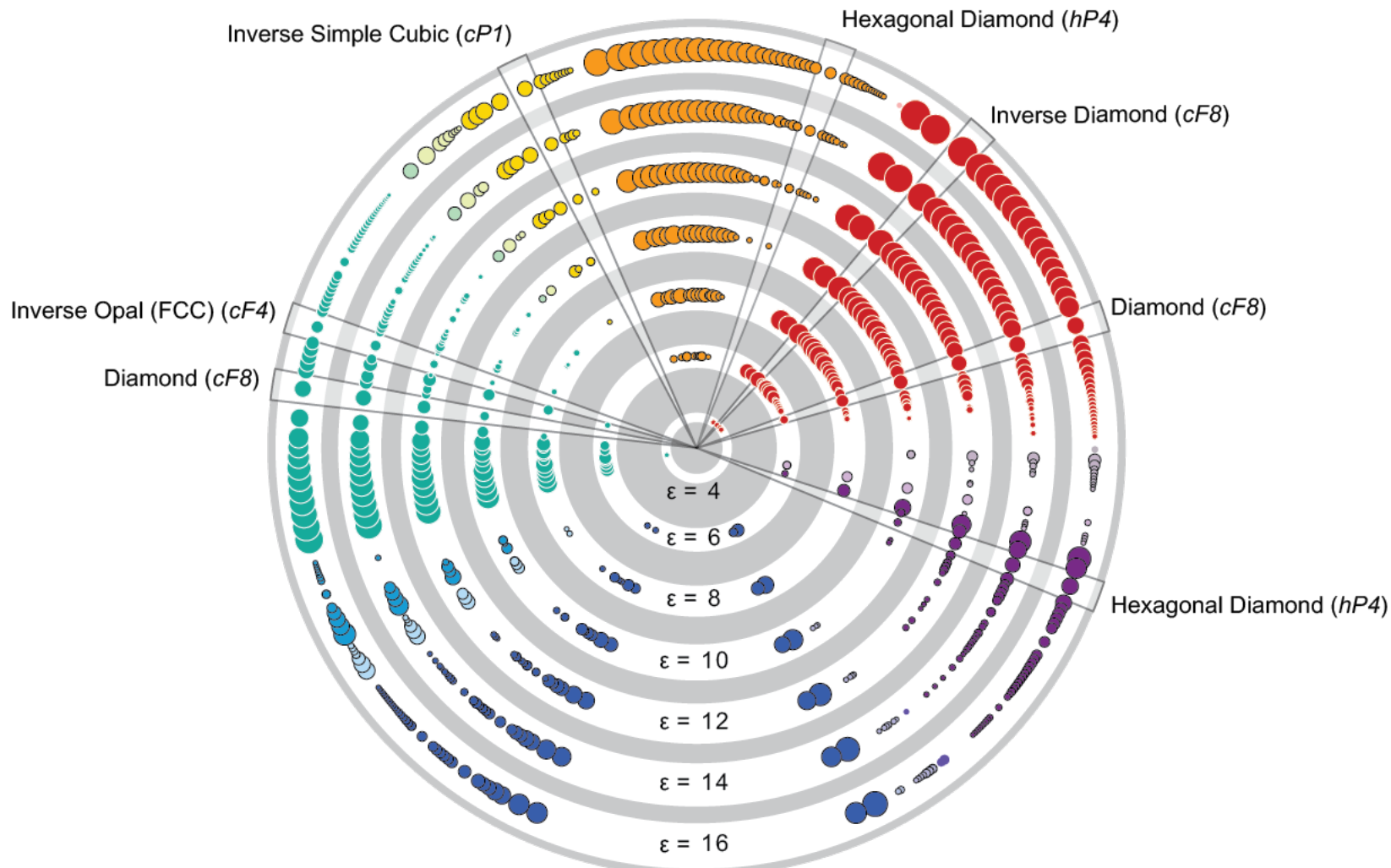
351 Photonic
“Templates”

474 Unique Gaps

Database of Photonic Crystals:
<https://glotzerlab.engin.umich.edu/photonics/index.html>

Appendix of Band Structures:
<https://deepblue.lib.umich.edu/handle/2027.42/153520>

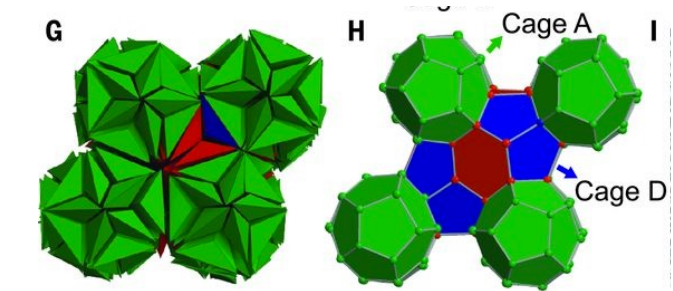
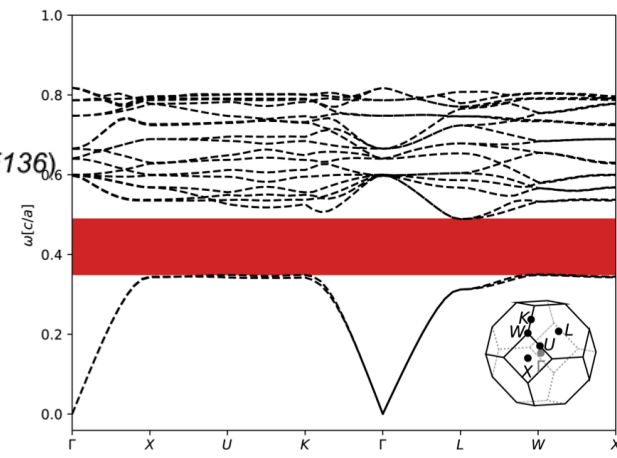
Each circle represents the maximum gap (circle size) found for a given template (radius), dielectric contrast (ring), and band location (color).



Each circle represents the maximum gap (circle size) found for a given template (radius), dielectric contrast (ring), and band location (color).

Inverse Clathrate-II

Maximum Gap: 33.9%

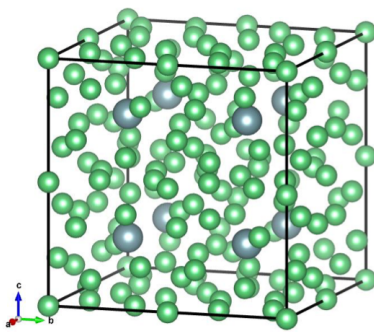
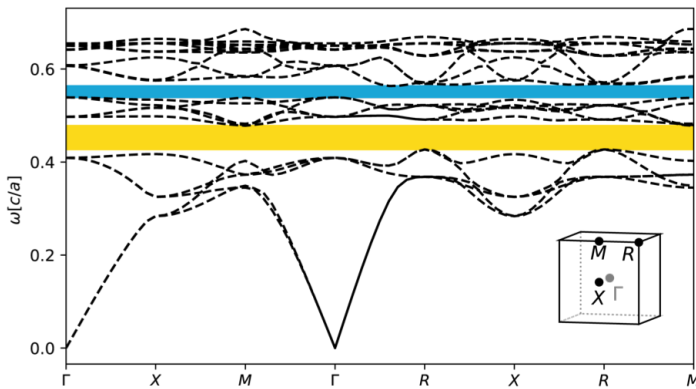


Clathrate colloidal crystals.

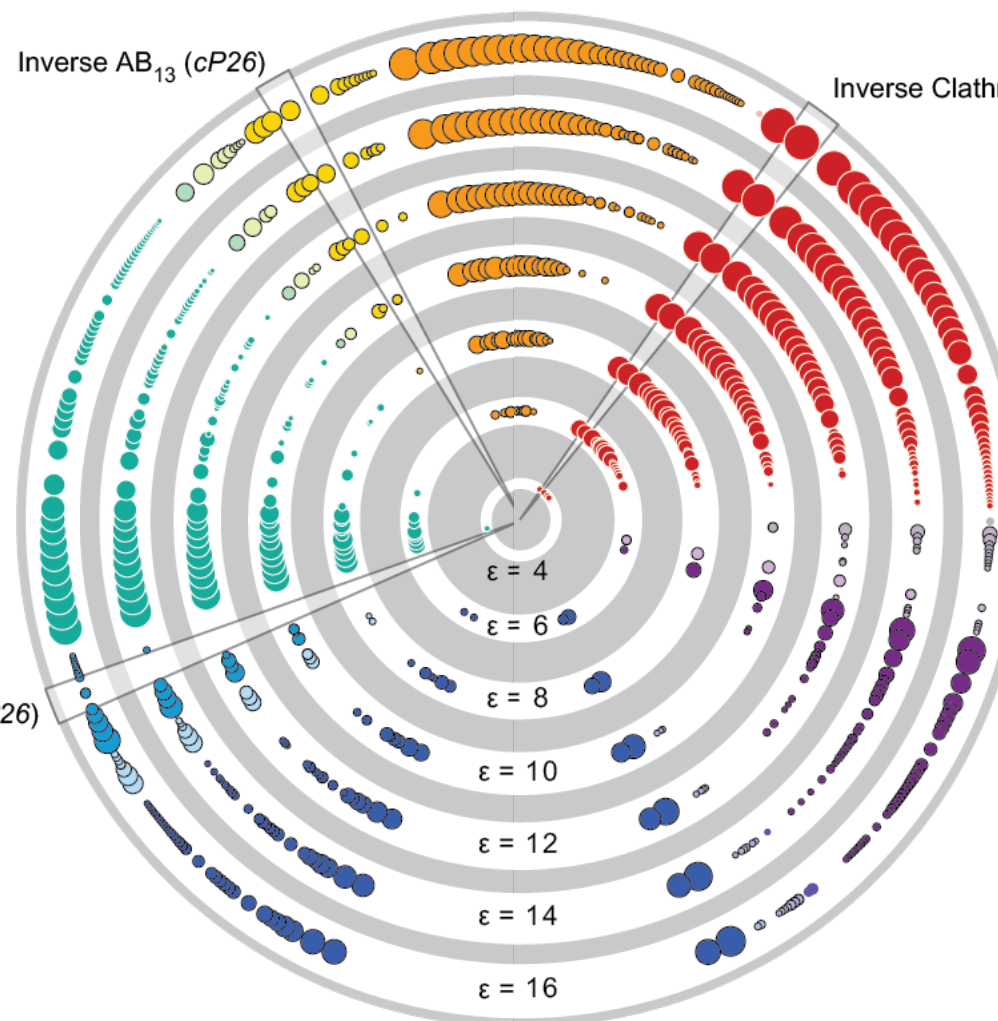
Lin, H., Lee, S., Sun, L., Spellings, M., Engel, M., Glotzer, S. C., & Mirkin, C. A. Science, 355(6328), 931-935.

Inverse AB₁₃

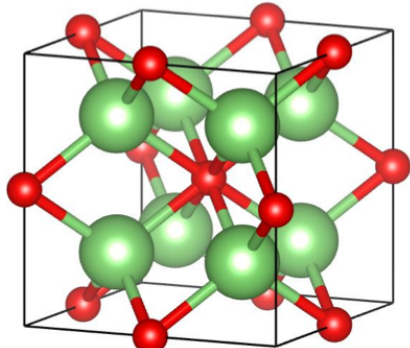
Maximum Gaps: 13.3% (Gaps 5-6),
4.78% (Gaps 10-11)



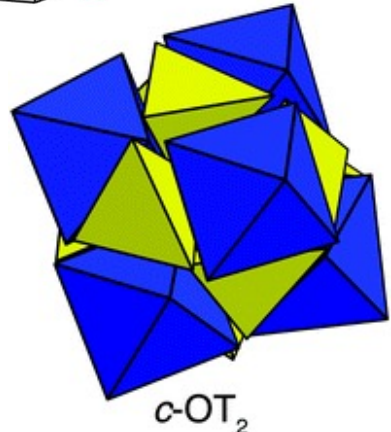
Inverse AB₁₃ (cP26)



Each circle represents the maximum gap (circle size) found for a given template (radius), dielectric contrast (ring), and band location (color).

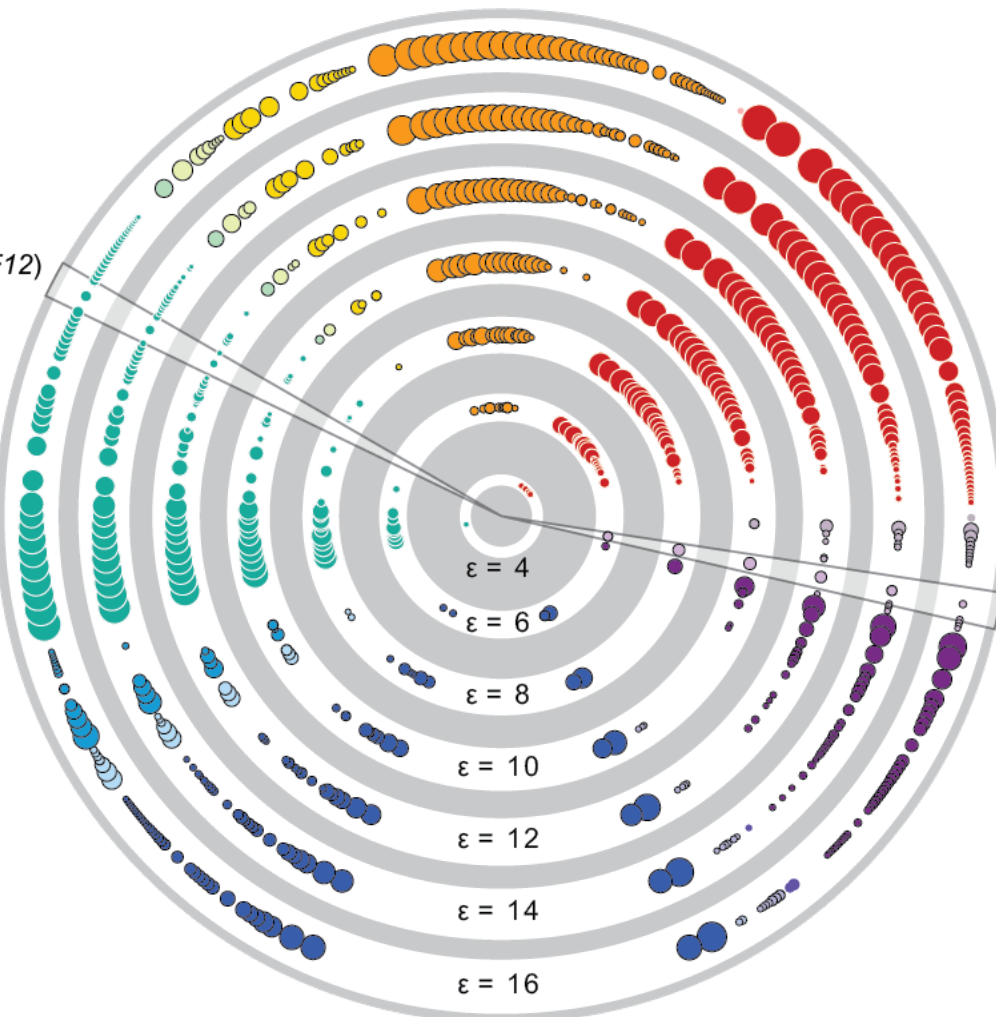


Lithium Oxide (*cF*12)



c-OT₂

Self-assembly of a space-tessellating structure in the binary system of hard tetrahedra and octahedra.
Cadotte, Andrew T., et al.
Soft matter 12.34 (2016): 7073-7078.



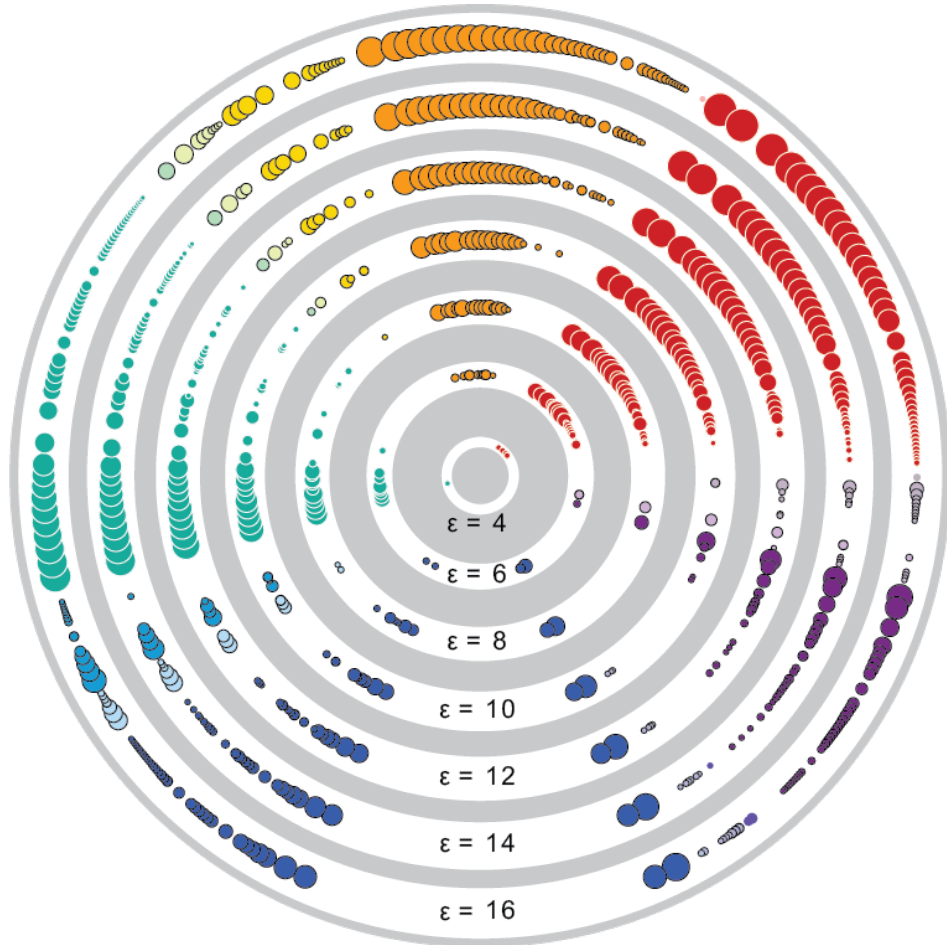
The lithium-oxide structure (a.k.a. Fluorite, *c*-OT₂, and F-RD) exhibits photonic anomalies, including a band gap that is largest at lower dielectric contrast.

Lithium Oxide (*cF*12)



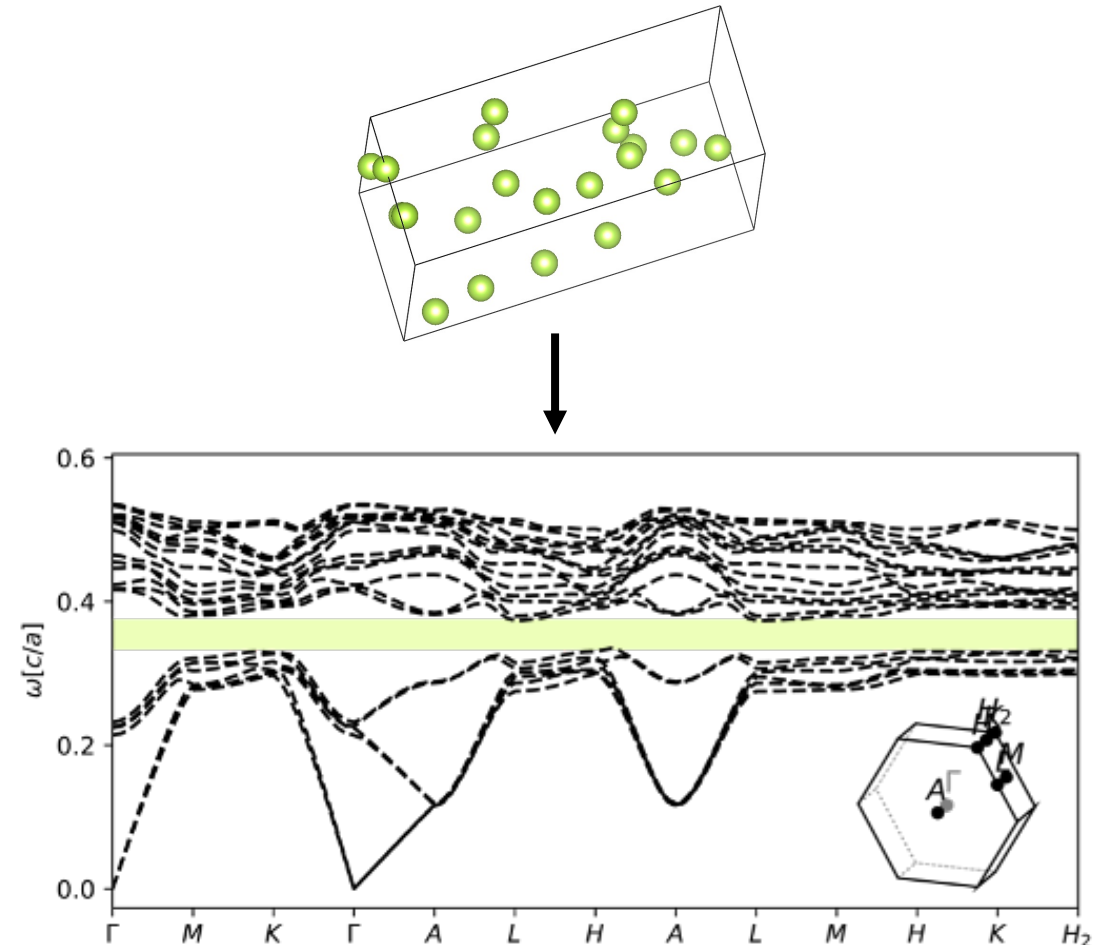
Each circle represents the maximum gap (circle size) found for a given template (radius), dielectric contrast (ring), and band location (color).

How else can we use this large dataset?



Database of Photonic Crystals:
<https://glotzerlab.engin.umich.edu/photonics/index.html>

November 7, 2021



AIChE

10

Generalized Neural-Network Representation of High-Dimensional Potential-Energy Surfaces

Jörg Behler and
Department of Chemistry and Applied Biosciences, ETH Zurich,
(Received 27 September 2006)

The accurate description of chemical processes methods like density-functional theory (DFT), in this Letter we introduce a new kind of neural-network which provides the energy and forces as a function is several orders of magnitude faster than DFT. The silicon and compared with empirical potentials at types of periodic and nonperiodic systems.

DOI: 10.1103/PhysRevLett.98.146401

The reliability of molecular dynamics (MD) or Monte Carlo (MC) simulations depends crucially on the accuracy of the underlying potential-energy surface (PES). *Ab initio* methods based on density-functional theory [1] (DFT) provide the most accurate PESs, but they are computationally very demanding and even on the most advanced platforms *ab initio* MD simulations are limited to tens of picoseconds and a few thousand atoms. This is the reason for the continuing popularity of empirical potential which provide fast access to energy and forces. However the construction of reliable empirical potentials is a difficult and lengthy process which usually relies on fitting the parameters of a guessed, physically motivated simple function form for the interaction potential. This can lead to qualitatively wrong predictions when it comes to cases in which the assumed functional form is not appropriate. The database used in the fitting can include experiments or theoretical data and even the forces obtained in an *ab initio* MD run [2–4].

In this Letter we present a generalized neural-network (NN) method for describing DFT-based PESs which have *ab initio* accuracy and are capable of describing all types of bonding. The method overcomes the limitations that have so far limited the use of NNs to low-dimensional systems [5,6]. This is achieved by combining NN precision and flexibility with a PES representation that is inspired by empirical potentials. The resulting many-body potentials are a function of all atomic coordinates and can be used in systems of arbitrary size. We apply our ideas to the construction of an NN-based many-body potential for bulk silicon. Constructing an empirical potential for Si that is valid across the phase diagram has proved to be a frustrating challenge for conventional empirical potentials. Our neural networks work in the solid, liquid, and in the liquid metallic phases. In addition we can reproduce the small energy differences between the different high-pressure phases of crystalline Si.

Neural networks are biology-inspired algorithms that provide an accurate tool for the representation of arbitrary functions. Given a number of points in which the value of

0031-9007/07/98(14)/146401(4)

146401

PRL 104, 136403 (2010)

PHYSICAL REVIEW LETTERS

week ending
2 APRIL 2010

Gaussian Approximation Potentials: The Accuracy of Quantum Mechanics, without the Electrons

Albert P. Bartók,^{1,4} Risi Kondor,²
Cavendish Laboratory, University of Cambridge, J.J.T.1

Risi Kondor,²
Center for the Mathematics of Information, California Institute of Technology, Pasadena, CA 91109, USA

Gábor Csányi,¹
Engineering Laboratory, University of Cambridge, Trumpington Street, Cambridge, CB3 9EW, UK

(Received 1 October 2009)

We introduce a class of interatomic potentials consisting of the energies and forces experienced by atoms. The models do not have a fixed functional form, but they are systematically built from bulk crystals, and test it by calculating properties at the construction of the long molecular dynamics trajectories. This is the reason for the continuing popularity of empirical potential which provide fast access to energy and forces. However the construction of reliable empirical potentials is a difficult and lengthy process which usually relies on fitting the parameters of a guessed, physically motivated simple function form for the interaction potential. This can lead to qualitatively wrong predictions when it comes to cases in which the assumed functional form is not appropriate. The database used in the fitting can include experiments or theoretical data and even the forces obtained in an *ab initio* MD run [2–4].

In this Letter we present a generalized neural-network (NN) method for describing DFT-based PESs which have *ab initio* accuracy and are capable of describing all types of bonding. The method overcomes the limitations that have so far limited the use of NNs to low-dimensional systems [5,6]. This is achieved by combining NN precision and flexibility with a PES representation that is inspired by empirical potentials. The resulting many-body potentials are a function of all atomic coordinates and can be used in systems of arbitrary size. We apply our ideas to the construction of an NN-based many-body potential for bulk silicon. Constructing an empirical potential for Si that is valid across the phase diagram has proved to be a frustrating challenge for conventional empirical potentials. Our neural networks work in the solid, liquid, and in the liquid metallic phases. In addition we can reproduce the small energy differences between the different high-pressure phases of crystalline Si.

Neural networks are biology-inspired algorithms that provide an accurate tool for the representation of arbitrary functions. Given a number of points in which the value of

0031-9007/10/104(13)/136403(4)

136403

PHYSICAL REVIEW LETTERS

week ending
2 APRIL 2010

On representing chemical environments

Albert P. Bartók,^{1,4} Risi Kondor,²
Cavendish Laboratory, University of Cambridge, J.J.T.1

Risi Kondor,²
Center for the Mathematics of Information, California Institute of Technology, Pasadena, CA 91109, USA

Gábor Csányi,¹
Engineering Laboratory, University of Cambridge, Trumpington Street, Cambridge, CB3 9EW, UK

(Received 1 December 2012, published online in Phys. Rev. Lett. 109, 016403 (2012))

We review some recently published methods to represent chemical environments. We show that periodic environments have a quantitatively different behavior than small clusters. We quantitatively show that the environments converge to very different rates. We also overlap of atom positions, that sidesteps these difficulties. We also discuss the performance of various representations by little clusters and the bulk crystal.

DOI: 10.1103/PhysRevLett.104.136403

Atomic scale modeling of materials is now routinely and widely applied, and encompasses a range of techniques from exact quantum chemical methods [1] through density functional theory (DFT) [2] and semiempirical quantum mechanics [3] to classical molecular dynamics [4]. The associated trade-offs in accuracy and computational cost are well known. Arguably, there is a gap between models that treat electrons explicitly and those that do not. Models in the former class are in practice limited to handling a few thousand atoms, while the simple analytic interatomic potentials are limited in accuracy, regardless of how they are parameterized. The panels in the top row of Fig. 1 illustrate the typical performance of analytic potentials in bulk systems. Periodic boundary conditions are generally regarded as adequate for describing these bulk phases show significant deviation from the quantum mechanical potential energy surface. This in turn gives rise to significant errors in predicting properties such as elastic constants and phonon spectra.

In this Letter we are concerned with the problem of modeling the Born-Oppenheimer potential energy surface (PES) of a set of atoms, but without recourse to simulating the electron motion. We only require a representation to model the bulk phases of carbon, silicon, germanium, iron, and gallium nitride, using a unified framework. Even such single-phase potentials could be useful for calculating physical properties, e.g., the thermal expansion coefficient, the phonon contribution to the thermal conductivity, the temperature dependence of the phonon modes, or as part of hybrid schemes [5].

The first key insight is that this is actually practicable: the reason that interatomic potentials are at all useful is that the PES is a relatively smooth function of the nuclear coordinates. Improving potential modeling is difficult not

by inventing more complex representations, but by specifying the position of each atom in a Cartesian coordinate system provides a simple and unequivocal description of atomic configurations; it is not directly suitable for making comparisons between structures: the list of coordinates is ordered arbitrarily and two structures might be mapped to each other by a rotation, reflection, or translation so that two different lists of coordinates, in fact, represent the same or very similar structures. A good representation is invariant with respect to permutational, rotational, reflectional, and translational symmetries, while retaining the faithfulness of the Cartesian representation. In particular, a system of invariant descriptors q_1, q_2, \dots, q_m is said to be complete if it uniquely defines the atom positions, in fact, up to symmetries. It would be incomplete if it contains spurious descriptors in the sense that a proper subset of $\{q_1, q_2, \dots, q_m\}$ is, by itself, complete. If a representation is complete, then

1098-0121/2013/87(18)/184115(16)

184

See supplementary material for details about the choice of basis functions and the calculation of the energy difference.

¹Number of graph nodes, ²Number of graphs, ³Number of graphs corresponding to a molecule containing a single topological component, ⁴Number of molecules obtained from the graphs by combined enumeration of unsaturations and heteroatoms and satisfying chemical stability and symmetry requirements. *Molecules are defined as a set of connected components of the graph. **Molecules are defined as a set of connected components of the graph. ***Molecules are defined as a set of connected components of the graph. ****Molecules are defined as a set of connected components of the graph. *****Molecules are defined as a set of connected components of the graph. [†]This database was computed in parallel on a 500-node cluster (see the Supporting Information for details).

[†]This database was computed in parallel on a 500-node cluster (see the Supporting Information for details).

[‡]Number of graph nodes, [§]Number of graphs, [¶]Number of graphs corresponding to a molecule containing a single topological component, ^{||}Number of molecules obtained from the graphs by combined enumeration of unsaturations and heteroatoms and satisfying chemical stability and symmetry requirements. *Molecules are defined as a set of connected components of the graph. **Molecules are defined as a set of connected components of the graph. ***Molecules are defined as a set of connected components of the graph. ****Molecules are defined as a set of connected components of the graph. *****Molecules are defined as a set of connected components of the graph. ^{††}This database was computed in parallel on a 500-node cluster (see the Supporting Information for details).

^{††}This database was computed in parallel on a 500-node cluster (see the Supporting Information for details).

^{‡‡}This database was computed in parallel on a 500-node cluster (see the Supporting Information for details).

^{¶¶}This database was computed in parallel on a 500-node cluster (see the Supporting Information for details).

^{||||}This database was computed in parallel on a 500-node cluster (see the Supporting Information for details).

^{*****}This database was computed in parallel on a 500-node cluster (see the Supporting Information for details).

^{*****}This database was computed in parallel on a 500-node cluster (see the Supporting Information for details).

^{*****}This database was computed in parallel on a 500-node cluster (see the Supporting Information for details).

^{*****}This database was computed in parallel on a 500-node cluster (see the Supporting Information for details).

^{*****}This database was computed in parallel on a 500-node cluster (see the Supporting Information for details).

^{*****}This database was computed in parallel on a 500-node cluster (see the Supporting Information for details).

^{*****}This database was computed in parallel on a 500-node cluster (see the Supporting Information for details).

^{*****}This database was computed in parallel on a 500-node cluster (see the Supporting Information for details).

^{*****}This database was computed in parallel on a 500-node cluster (see the Supporting Information for details).

^{*****}This database was computed in parallel on a 500-node cluster (see the Supporting Information for details).

^{*****}This database was computed in parallel on a 500-node cluster (see the Supporting Information for details).

^{*****}This database was computed in parallel on a 500-node cluster (see the Supporting Information for details).

^{*****}This database was computed in parallel on a 500-node cluster (see the Supporting Information for details).

^{*****}This database was computed in parallel on a 500-node cluster (see the Supporting Information for details).

^{*****}This database was computed in parallel on a 500-node cluster (see the Supporting Information for details).

^{*****}This database was computed in parallel on a 500-node cluster (see the Supporting Information for details).

^{*****}This database was computed in parallel on a 500-node cluster (see the Supporting Information for details).

^{*****}This database was computed in parallel on a 500-node cluster (see the Supporting Information for details).

^{*****}This database was computed in parallel on a 500-node cluster (see the Supporting Information for details).

^{*****}This database was computed in parallel on a 500-node cluster (see the Supporting Information for details).

^{*****}This database was computed in parallel on a 500-node cluster (see the Supporting Information for details).

^{*****}This database was computed in parallel on a 500-node cluster (see the Supporting Information for details).

^{*****}This database was computed in parallel on a 500-node cluster (see the Supporting Information for details).

^{*****}This database was computed in parallel on a 500-node cluster (see the Supporting Information for details).

^{*****}This database was computed in parallel on a 500-node cluster (see the Supporting Information for details).

^{*****}This database was computed in parallel on a 500-node cluster (see the Supporting Information for details).

^{*****}This database was computed in parallel on a 500-node cluster (see the Supporting Information for details).

^{*****}This database was computed in parallel on a 500-node cluster (see the Supporting Information for details).

^{*****}This database was computed in parallel on a 500-node cluster (see the Supporting Information for details).

^{*****}This database was computed in parallel on a 500-node cluster (see the Supporting Information for details).

^{*****}This database was computed in parallel on a 500-node cluster (see the Supporting Information for details).

^{*****}This database was computed in parallel on a 500-node cluster (see the Supporting Information for details).

^{*****}This database was computed in parallel on a 500-node cluster (see the Supporting Information for details).

^{*****}This database was computed in parallel on a 500-node cluster (see the Supporting Information for details).

^{*****}This database was computed in parallel on a 500-node cluster (see the Supporting Information for details).

^{*****}This database was computed in parallel on a 500-node cluster (see the Supporting Information for details).

^{*****}This database was computed in parallel on a 500-node cluster (see the Supporting Information for details).

^{*****}This database was computed in parallel on a 500-node cluster (see the Supporting Information for details).

^{*****}This database was computed in parallel on a 500-node cluster (see the Supporting Information for details).

^{*****}This database was computed in parallel on a 500-node cluster (see the Supporting Information for details).

^{*****}This database was computed in parallel on a 500-node cluster (see the Supporting Information for details).

^{*****}This database was computed in parallel on a 500-node cluster (see the Supporting Information for details).

^{*****}This database was computed in parallel on a 500-node cluster (see the Supporting Information for details).

^{*****}This database was computed in parallel on a 500-node cluster (see the Supporting Information for details).

^{*****}This database was computed in parallel on a 500-node cluster (see the Supporting Information for details).

^{*****}This database was computed in parallel on a 500-node cluster (see the Supporting Information for details).

^{*****}This database was computed in parallel on a 500-node cluster (see the Supporting Information for details).

^{*****}This database was computed in parallel on a 500-node cluster (see the Supporting Information for details).

^{*****}This database was computed in parallel on a 500-node cluster (see the Supporting Information for details).

^{*****}This database was computed in parallel on a 500-node cluster (see the Supporting Information for details).

^{*****}This database was computed in parallel on a 500-node cluster (see the Supporting Information for details).

^{*****}This database was computed in parallel on a 500-node cluster (see the Supporting Information for details).

^{*****}This database was computed in parallel on a 500-node cluster (see the Supporting Information for details).

^{*****}This database was computed in parallel on a 500-node cluster (see the Supporting Information for details).

^{*****}This database was computed in parallel on a 500-node cluster (see the Supporting Information for details).

^{*****}This database was computed in parallel on a 500-node cluster (see the Supporting Information for details).

^{*****}This database was computed in parallel on a 500-node cluster (see the Supporting Information for details).

^{*****}This database was computed in parallel on a 500-node cluster (see the Supporting Information for details).

^{*****}This database was computed in parallel on a 500-node cluster (see the Supporting Information for details).

^{*****}This database was computed in parallel on a 500-node cluster (see the Supporting Information for details).

^{*****}This database was computed in parallel on a 500-node cluster (see the Supporting Information for details).

^{*****}This database was computed in parallel on a 500-node cluster (see the Supporting Information for details).

^{*****}This database was computed in parallel on a 500-node cluster (see the Supporting Information for details).

^{*****}This database was computed in parallel on a 500-node cluster (see the Supporting Information for details).

^{*****}This database was computed in parallel on a 500-node cluster (see the Supporting Information for details).

^{*****}This database was computed in parallel on a 500-node cluster (see the Supporting Information for details).

^{*****}This database was computed in parallel on a 500-node cluster (see the Supporting Information for details).

^{*****}This database was computed in parallel on a 500-node cluster (see the Supporting Information for details).

^{*****}This database was computed in parallel on a 500-node cluster (see the Supporting Information for details).

^{*****}This database was computed in parallel on a 500-node cluster (see the Supporting Information for details).

^{*****}This database was computed in parallel on a 500-node cluster (see the Supporting Information for details).

^{*****}This database was computed in parallel on a 500-node cluster (see the Supporting Information for details).

^{*****}This database was computed in parallel on a 500-node cluster (see the Supporting Information for details).

^{*****}This database was computed in parallel on a 500-node cluster (see the Supporting Information for details).

^{*****}This database was computed in parallel on a 500-node cluster (see the Supporting Information for details).

^{*****}This database was computed in parallel on a 500-node cluster (see the Supporting Information for details).

^{*****}This database was computed in parallel on a 500-node cluster (see the Supporting Information for details).

^{*****}This database was computed in parallel on a 500-node cluster (see the Supporting Information for details).

^{*****}This database was computed in parallel on a 500-node cluster (see the Supporting Information for details).

^{*****}This database was computed in parallel on a 500-node cluster (see the Supporting Information for details).

^{*****}This database was computed in parallel on a 500-node cluster (see the Supporting Information for details).

^{*****}This database was computed in parallel on a 500-node cluster (see the Supporting Information for details).

^{*****}This database was computed in parallel on a 500-node cluster (see the Supporting Information for details).

^{*****}This database was computed in parallel on a 500-node cluster (see the Supporting Information for details).

^{*****}This database was computed in parallel on a 500-node cluster (see the Supporting Information for details).

^{*****}This database was computed in parallel on a 500-node cluster (see the Supporting Information for details).

^{*****}This database was computed in parallel on a 500-node cluster (see the Supporting Information for details).

^{*****}This database was computed in parallel on a 500-node cluster (see the Supporting Information for details).

^{*****}This database was computed in parallel on a 500-node cluster (see the Supporting Information for details).

^{*****}This database was computed in parallel on a 500-node cluster (see the Supporting Information for details).

^{*****}This database was computed in parallel on a 500-node cluster (see the Supporting Information for details).

^{*****}This database was computed in parallel on a 500-node cluster (see the Supporting Information for details).

^{*****}This database was computed in parallel on a 500-node cluster (see the Supporting Information for details).

^{*****}This database was computed in parallel on a 500-node cluster (see the Supporting Information for details).

^{*****}This database was computed in parallel on a 500-node cluster (see the Supporting Information for details).

^{*****}This database was computed in parallel on a 500-node cluster (see the Supporting Information for details).

^{*****}This database was computed in parallel on a 500-node cluster (see the Supporting Information for details).

^{*****}This database was computed in parallel on a 500-node cluster (see the Supporting Information for details).

^{*****}This database was computed in parallel on a 500-node cluster (see the Supporting Information for details).

^{*****}This database was computed in parallel on a 500-node cluster (see the Supporting Information for details).

^{*****}This database was computed in parallel on a 500-node cluster (see the Supporting Information for details).

^{*****}This database was computed in parallel on a 500-node cluster (see the Supporting Information for details).

^{*****}This database was computed in parallel on a 500-node cluster (see the Supporting Information for details).

^{*****}This database was computed in parallel on a 500-node cluster (see the Supporting Information for details).

^{*****}This database was computed in parallel on a 500-node cluster (see the Supporting Information for details).

^{*****}This database was computed in parallel on a 500-node cluster (see the Supporting Information for details).

^{*****}This database was computed in parallel on a 500-node cluster (see the Supporting Information for details).

^{*****}This database was computed in parallel on a 500-node cluster (see the Supporting Information for details).

^{*****}This database was computed in parallel on a 500-node cluster (see the Supporting Information for details).

^{*****}This database was computed in parallel on a 500-node cluster (see the Supporting Information for details).

^{*****}This database was computed in parallel on a 500-node cluster (see the Supporting Information for details).

^{*****}This database was computed in parallel on a 500-node cluster (see the Supporting Information for details).

EPFL



COSMO
COMPUTATIONAL SCIENCE AND MODELLING



At time of presentation, this work was not yet published, please see
rosecersonsky.com for recent publications.



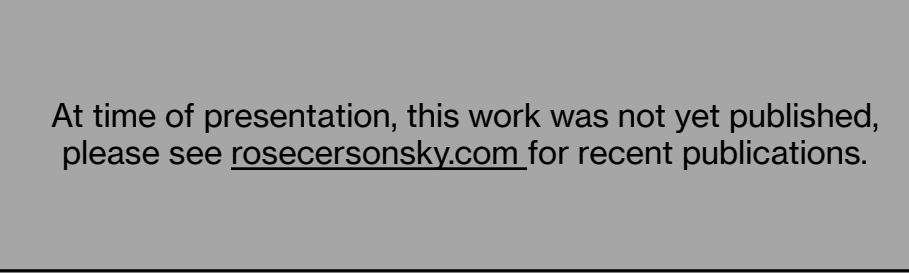
The Search for Novel Mesoscale Materials

Rose K. Cersonsky

Laboratory of Computational Science and Modeling (COSMO)
École Polytechnique Fédérale de Lausanne (EPFL)
Lausanne, Switzerland



At time of presentation, this work was not yet published,
please see rosecersonsky.com for recent publications.



Come see my last talk!
**203e - Improving Data
Sub-Selection for
Supervised Tasks with
Principal Covariates
Regression**

Monday, November 8,
2021
4:30 PM - 4:45 PM EDT
Marriott Copley Place -
Salon H/I



rosecersonsky.com